

Enzyme-Functionalized Cellulose Beads as a Promising Antimicrobial Material

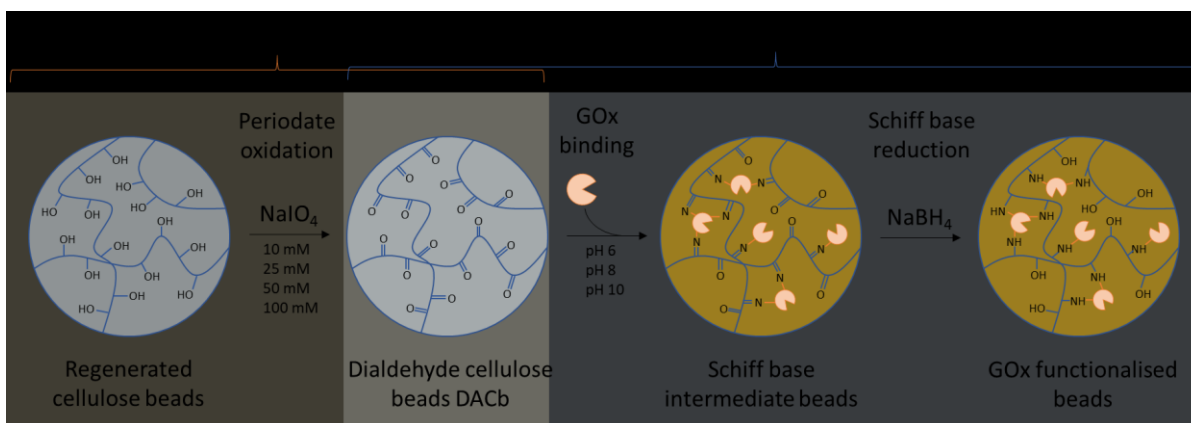
Davide Califano^{a,b}, Bethany Lee Patenall^{a,b}, Marco Kadowaki^a, Davide Mattia^c, Janet L. Scott^{a,b}, Karen J. Edler^a*

a. Department of Chemistry, University of Bath, Claverton Down, Bath, UK.

b. Centre for Sustainable Chemical Technologies, University of Bath, Claverton Down, Bath,
UK.

c. Department of Chemical Engineering, University of Bath, BA27AY, UK

Keywords: Cellulose, Glucose oxidase, enzyme immobilization, antimicrobial material,
biodegradable, beads, hydrogen peroxide, H₂O₂, antibiotic resistance.



Scheme 1. The general approach to creation of the enzyme-functionalized dialdehyde cellulose beads. Details are provided in the Experimental Section below.

Table 1. Degree of oxidation of cellulose in relation with the periodate concentration in the reaction vessel and periodate/cellulose molar ratio.

<i>Sample code</i>	<i>NaIO₄ conc. (mM)</i>	<i>NaIO₄ / Cellulose ratio (mol/mol)</i>	<i>Degree of oxidation (%)¹</i>	<i>Standard deviation</i>
<i>DACb-10</i>	10	0.07	4.13	0.30
<i>DACb-25</i>	25	0.17	7.42	0.50
<i>DACb-50</i>	50	0.34	11.20	0.93
<i>DACb-100</i>	100	0.68	19.56	1.32

¹ Degree of oxidation is expressed in moles of carbonyls per mole of anhydrous glucose units (AUG) as a percentage. The highest degree of oxidation (100 %) corresponds to a degree of substitution (DS) equal to 2 as periodate can oxidise only vicinal diols. Thus, only 2 out of 3 hydroxyl groups for each AUG.

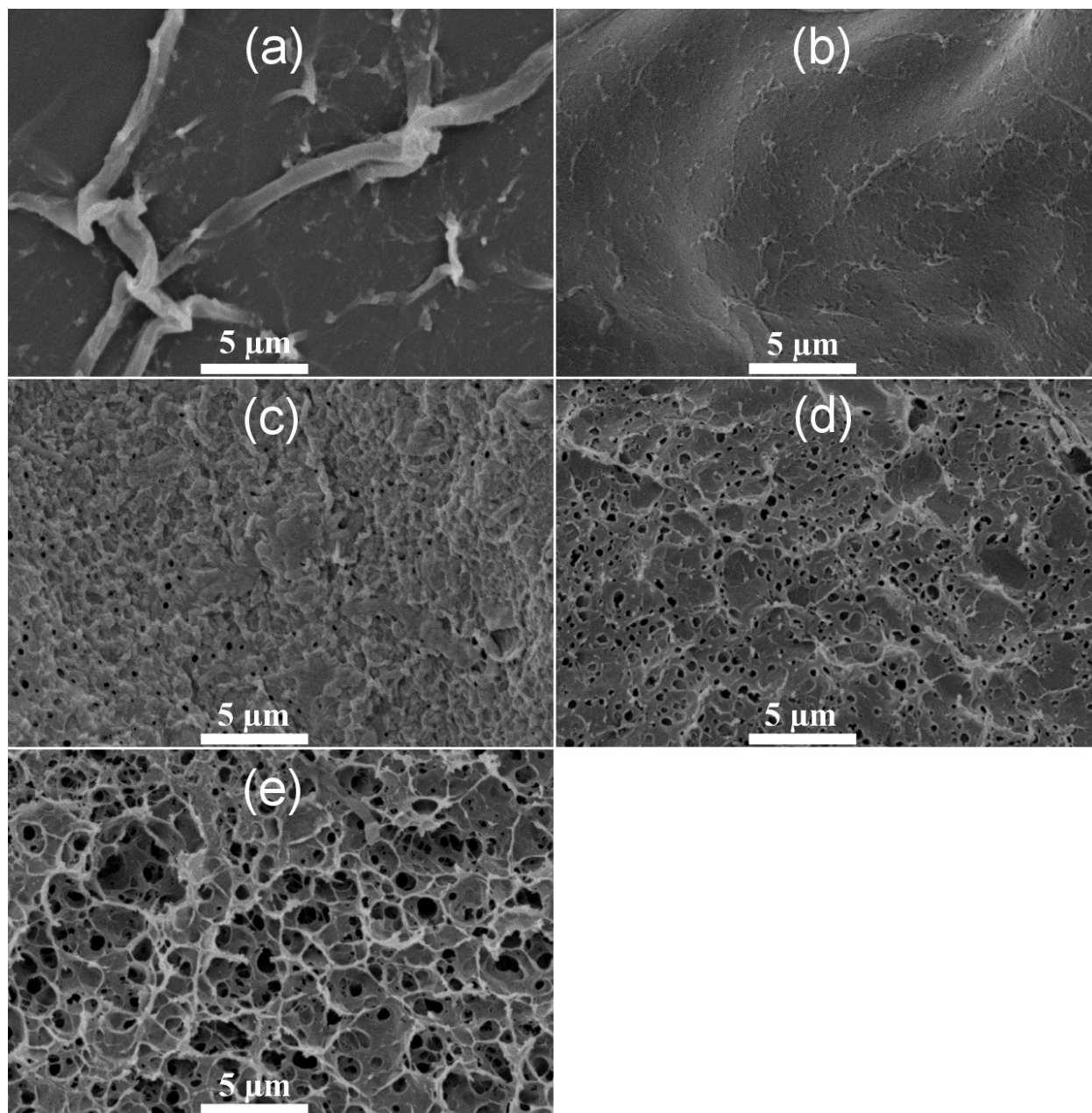


Figure 1. Cross-sections of DACb prior to functionalization. The SEM micrographs show the porosity of the beads after freeze-drying. The periodate oxidation of cellulose increases the preservation of a porous structure upon freeze-drying. From (a) to (e) DACb with different degrees of oxidation (DO), DACb-0, DACb-10, DACb-25, DACb-50 and DACb-100 respectively.

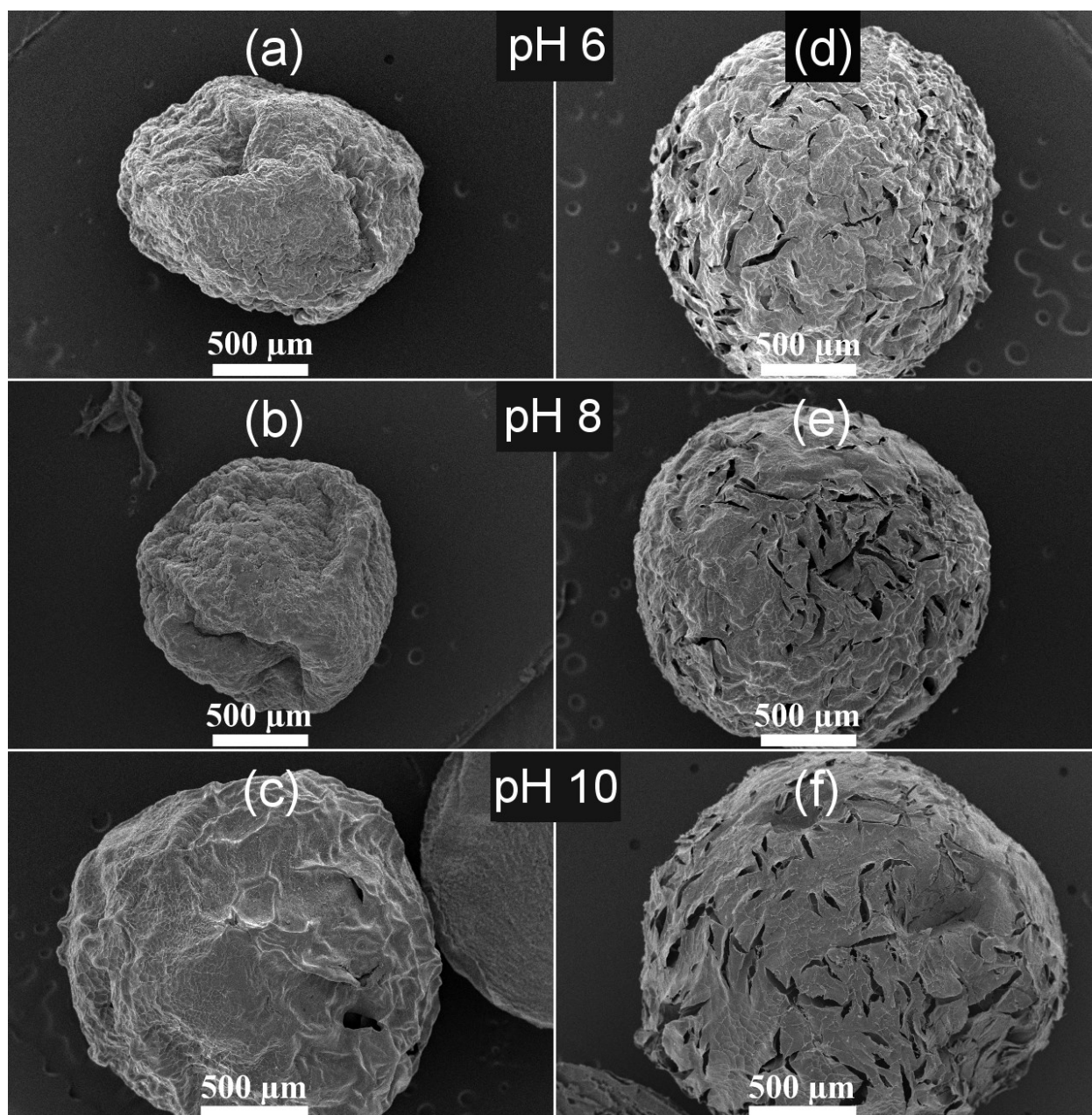
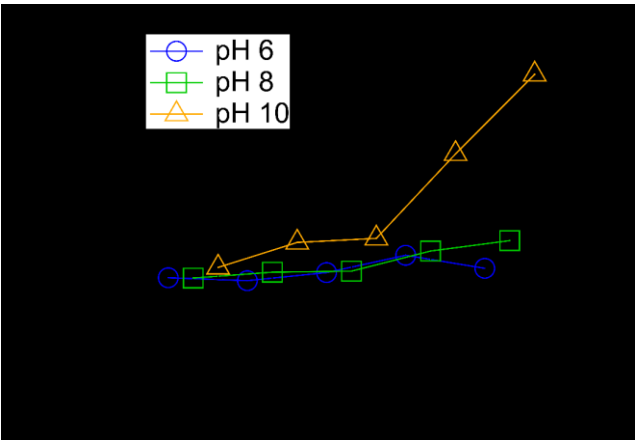


Figure 2. Scanning electron micrographs of beads exposed to different pH solutions. From (a) to (c) non-oxidised beads (controls), from (d) to (f) oxidised DACb-10. The photomicrographs show a different susceptibility to hornification upon freeze-drying. The control beads show a greater degree of cellulose aggregation and collapse compared to the DACb-10 (lowest degree of oxidation after reaction with periodate).

36



37

38

39

40

41

Figure 3. Functionalised beads resistance to mechanical uniaxial compression. The graph shows the differences in critical strain of oxidised beads when exposed at pH 6, 8 and 10 (blue, green and orange respectively). The oxidised beads' mechanical resistance to the compression is significantly affected only when exposed to alkaline pH. Error bars represent the standard deviation (n=3).

42

43

Table 2. ² Binding affinity constants (K_h) and R^2 of their fitting for GOx bound on DACb are reported.

Sample code	pH6		pH8		pH10	
	K_h	R^2	K_h	R^2	K_h	R^2
DACb - 0	21.58	0.97	14.06	0.92	66.55 *	0.89 *
DACb - 10	22.92	0.99	17.02	0.92	97.08	0.99
DACb - 25	22.62	0.97	21.23	0.96	105.25	0.97
DACb - 50	30.06	0.93	29.84	0.93	97.34	0.95
DACb - 100	37.35	0.94	42.62	0.91	123.96	0.91

44

² Enzyme was bound on beads with different degrees of oxidation at different pH to determine the binding affinity constants (K_h). * The K_h for control beads at pH 10 were calculated only using the first 3 points as the binding curve reaches a plateau.

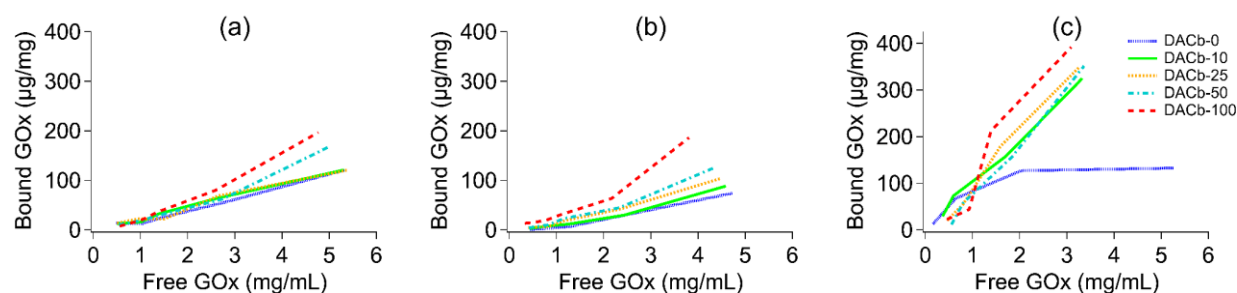


Figure 4. Binding isotherm plots. Binding affinity of GOx in beads with different DO during the binding step with enzyme solutions buffered at different pH. Binding at pH 6 (a), at pH 8 (b) and pH 10 (c). Each point represents the mean of independent samples (n=3).

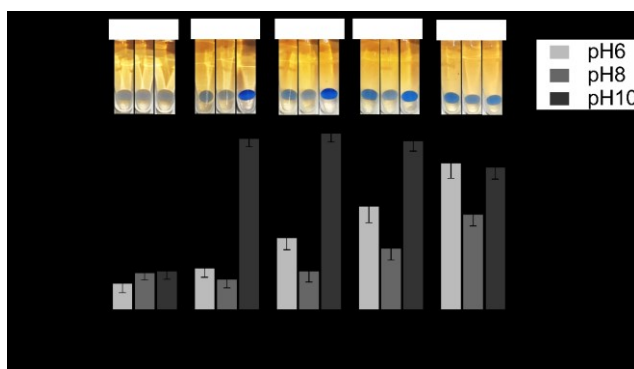


Figure 5. GOx content in DACb after binding at different pH and degree of oxidation. The graph shows the relative GOx content in the beads calculated extrapolating the grey intensity from images (insets above) after staining with Coomassie blue (Bradford reagent). The enzyme, dissolved in different buffered solutions at pH 6, 8 and 10, was bound in DACb with different DO values. The GOx content exhibits different trends after the whole immobilisation process (enzyme binding, NaBH₄ reduction and washing). Error bars represent the standard deviation (n=3).

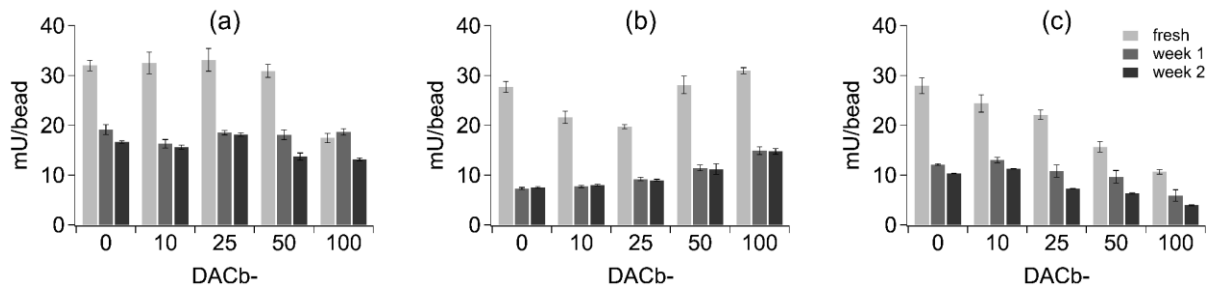


Figure 6. GOx activity upon storage. Activity of beads functionalised at pH6 (a), at pH 8 (b) and pH 10 (c) upon storage at 4 °C. Error bars represent the standard deviation (n=3).

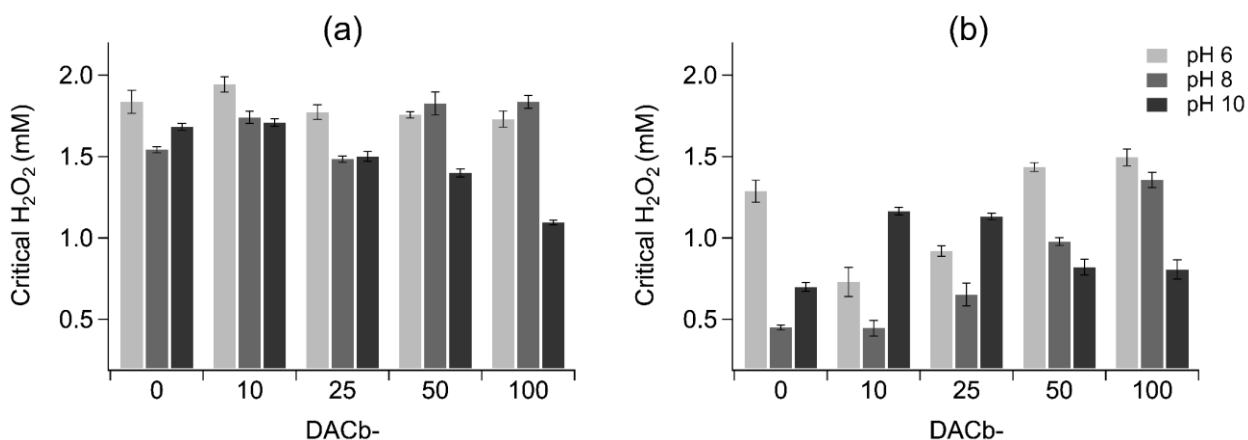


Figure 7. H₂O₂ critical concentration. Concentration of H₂O₂ reached after 24 hours of reaction in 10 mL of substrate of freshly functionalized beads (a) and after 14 days storage at 4 °C (b). Error bars represent the standard deviation (n=3).

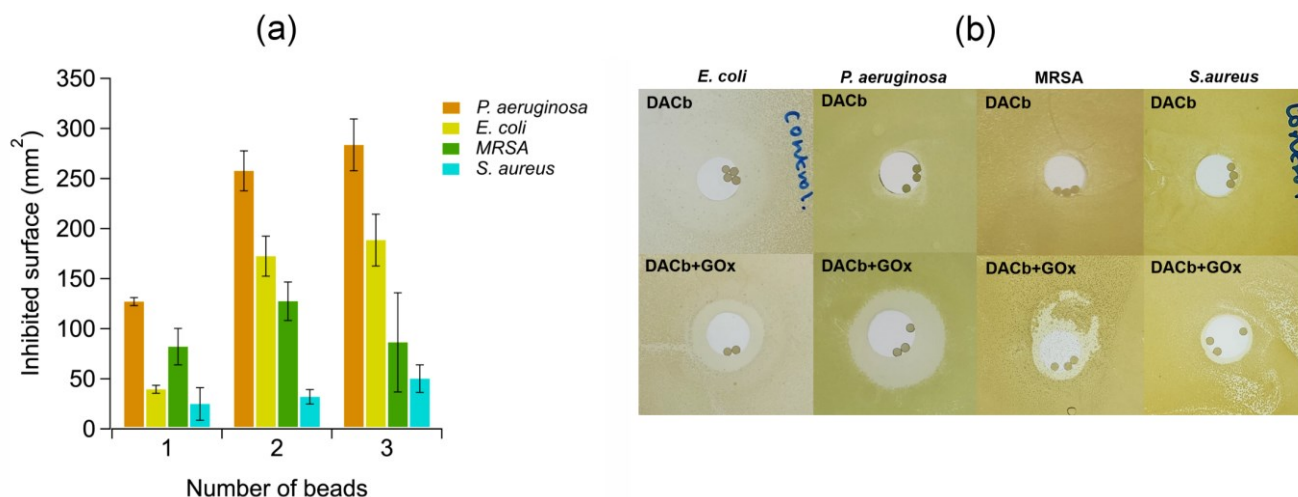
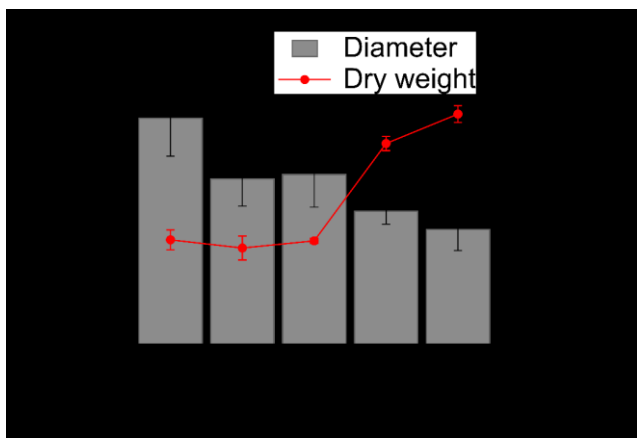


Figure 8. Inhibition halo assay. (a) The graph shows the surface inhibited by the functionalized DACb in the agar diffusion test. The amount of DACb used in the test does not influence the surface inhibited in MRSA (MRSA252) and *S. aureus* (H560), while it increases the surface inhibited in *P. aeruginosa* (PAO1) and *E. coli* (NCTC 10418) between 1 and 2 beads. Error bars represent the standard deviation (n=3). (b) The plates above represent the DACb prior GOx functionalization (controls). The plates below represent the DACb functionalized with GOx. All the bacteria used were inhibited by functionalized DACb and the highest inhibition was observed towards *P. aeruginosa* and *E. coli*.

Figure ESI 1: Beads size upon periodate oxidation. The beads diameter significantly decreased in cellulose beads with a higher degree of oxidation suggesting a structural rearrangement of the polymer network. Error bars represent the standard deviation obtained from (n=30).



81

82 Figure ESI 2: Uniaxial deformation test. The plots from (a) to (e) show the resistance to

83 compression of DACb-0, DACb-10, DACb-25, DACb-50 and DACb-100 respectively after

84 exposure at pH 6 (blue), 8 (green) and 10 (orange). All curves are characterized by an initial steady

85 increase, followed by a sharp peak of the axial force over the strain which represent the elastic

86 region and a strain-hardening region.

87

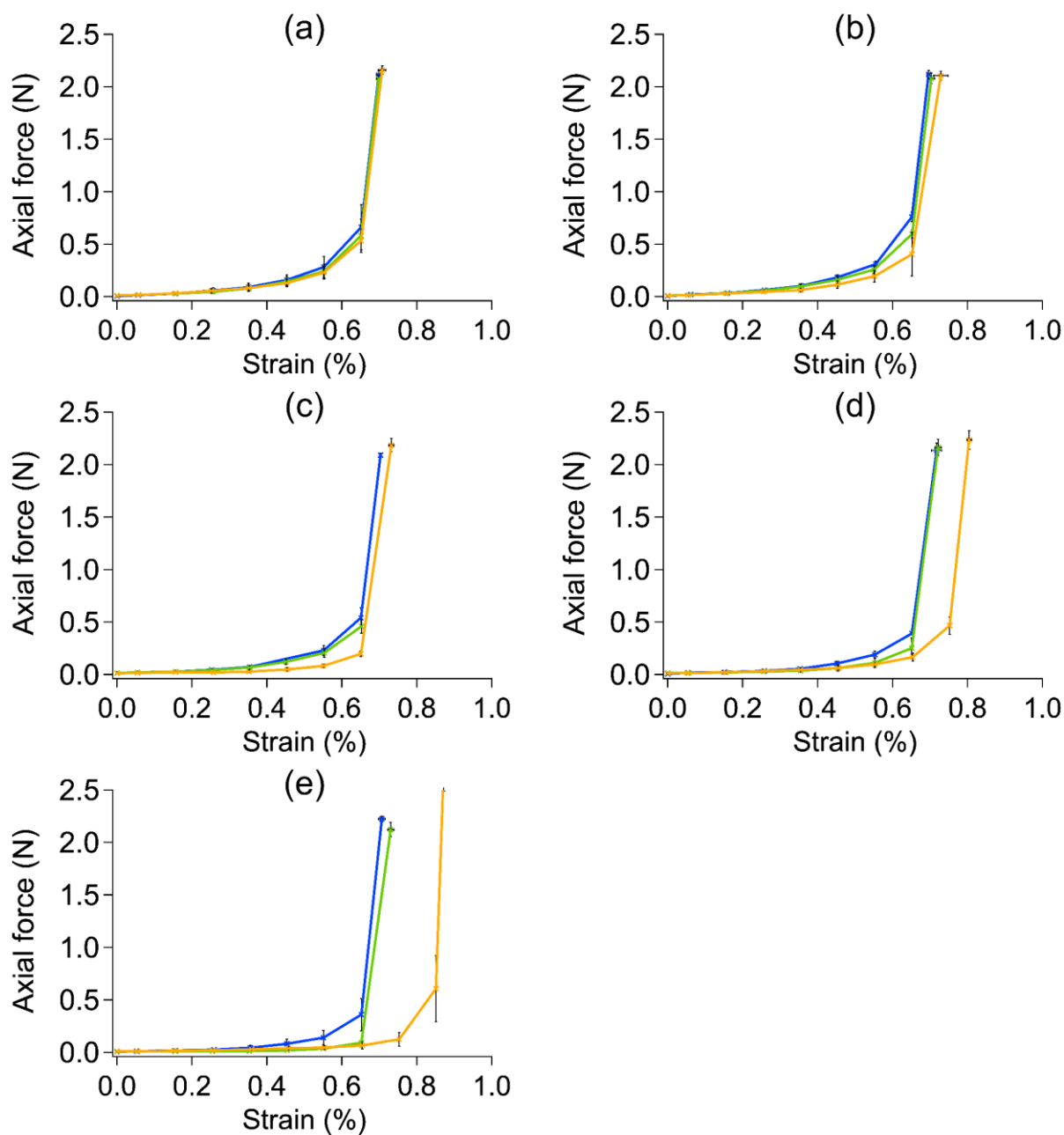
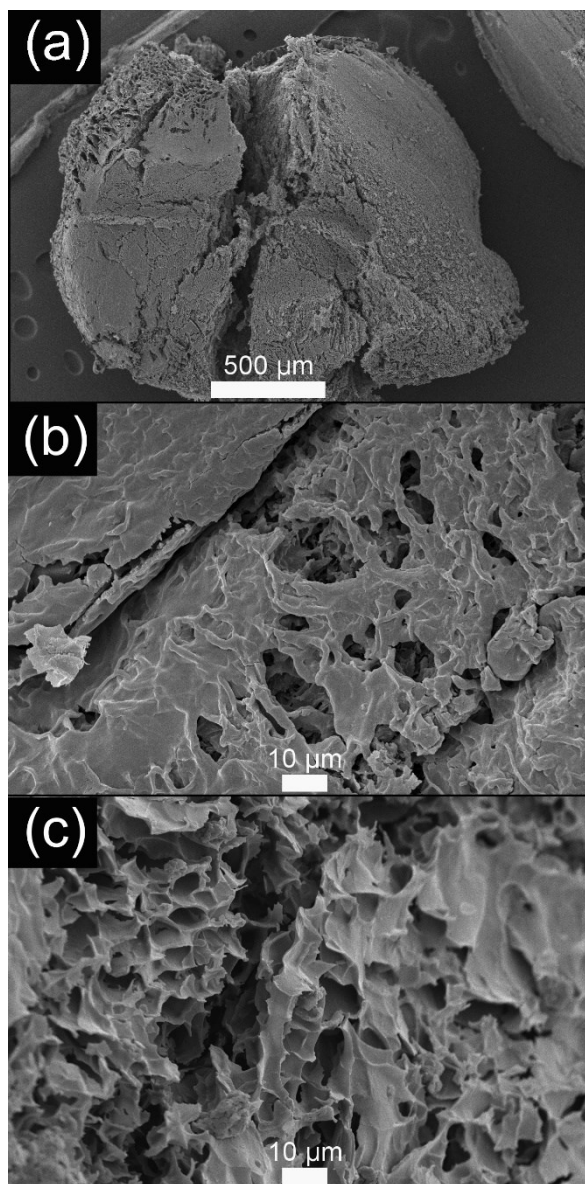


Figure ESI 3: Scanning electron micrographs of DACb-100 functionalized at pH 10. (a) The bead shows multiple fractures upon freeze-drying indicating structural damage of the cellulose network. (b) Structural damage of the internal structure and the outer layer bead of a single bead. (c) A magnified picture of the bead core showing the brittleness of the internal structure.



95

96 Figure ESI 4: Kinetic curves of DACb at different degree of oxidation and functionalized using
97 different pH. All H_2O_2 kinetic curves show a linear growth in the first 2.5 h followed by a flattening
98 and a saturation point. The plots from (a) to (e) display the H_2O_2 kinetics of DACb-0, DACb-10,
99 DACb-25, DACb-50 and DACb-100 respectively. Line colors represent DACb functionalized at

different, blue at pH 6, green at pH 8 and orange at pH 10. The shadows represent the standard deviation (n=3).

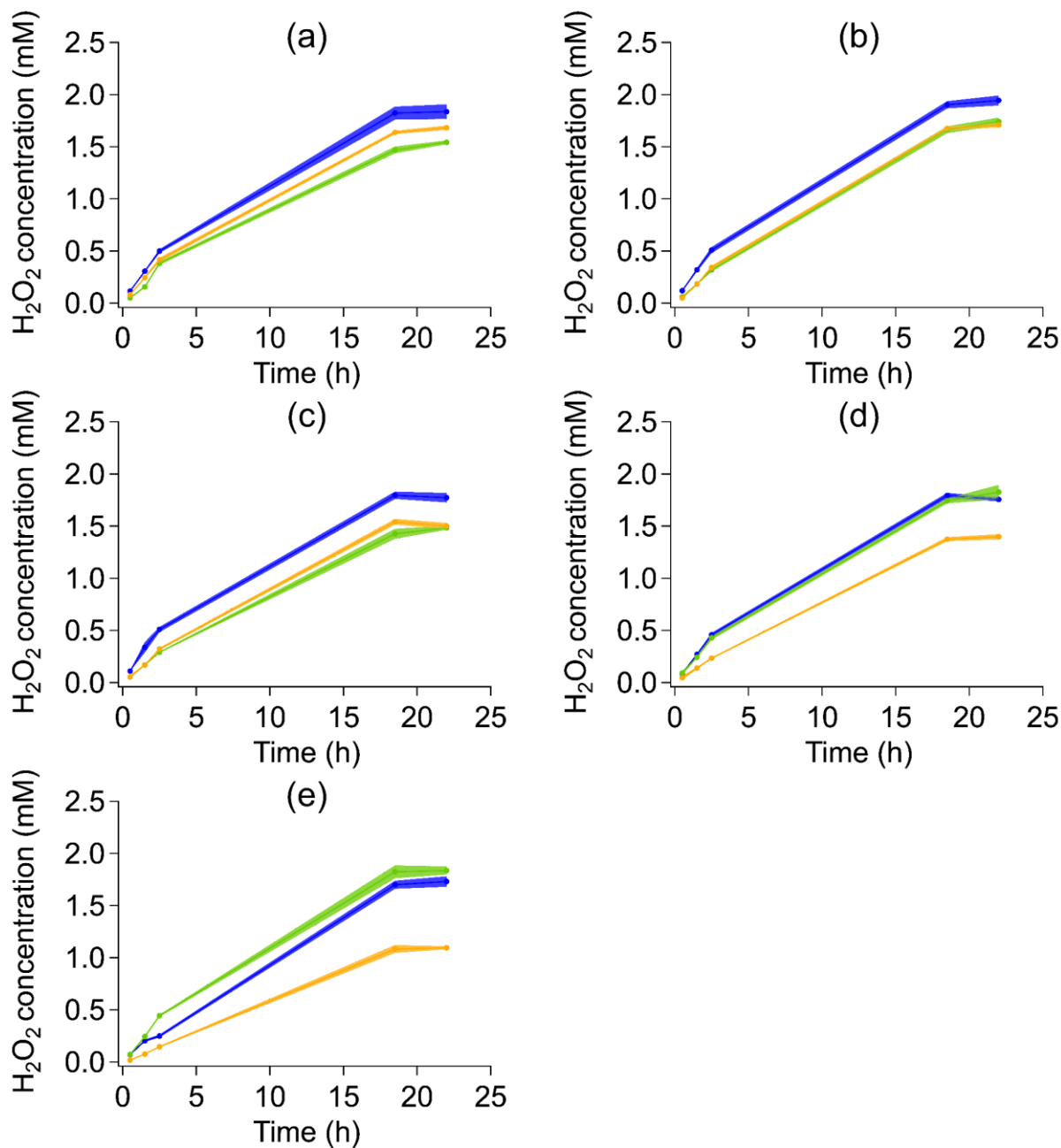


Figure ESI 5: Functionalized beads H_2O_2 release in a larger volume. The release of H_2O_2 from the functionalized beads increased linearly confirming that the GOx activity is not inhibited when

exposed to lower concentrations of H_2O_2 compared those reached in smaller volumes ($\approx 2 \text{ mM}$).
The shadows represent the standard deviation ($n=3$).

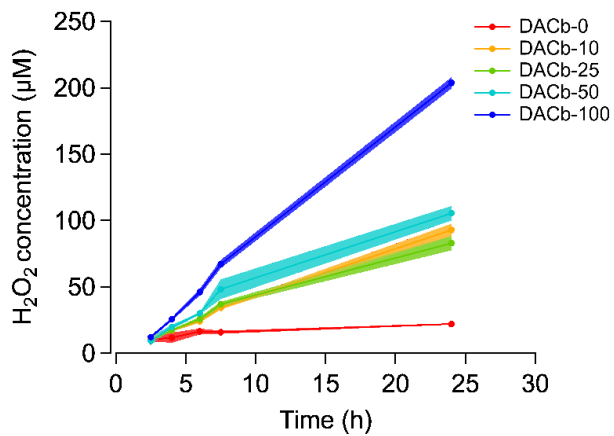
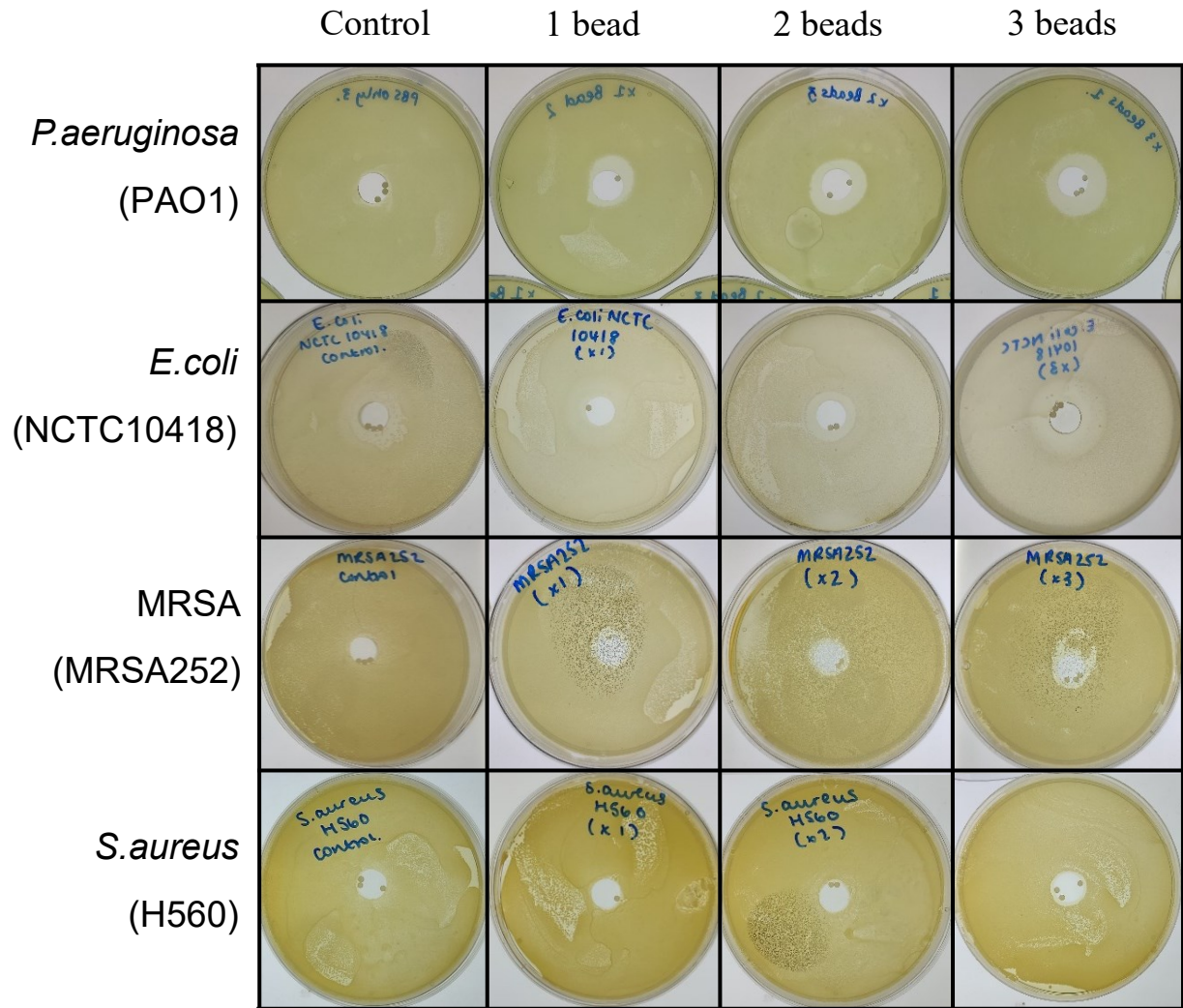
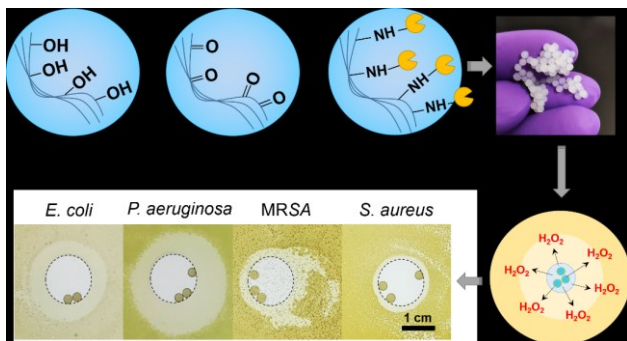


Figure ESI 6: Dose-dependent antimicrobial response of functionalized beads of the agar diffusion test. The control beads did not contain GOx while the other beads were oxidized DACb-100 functionalized with GOx at pH 6. All beads were incubated with a buffered solution (phosphate buffer, pH 6, 0.1M) containing 1 wt.% glucose.



126 Graphical abstract (TOC)



127